GROWTH CHARACTERISTICS OF CO-CR THIN FILMS FOR MAGNETIC RECORDING

B. G. DEMCZYK AND D. E. LAUGHLIN
Department of Metallurgical Engineering and Materials Science,Carnegie-Mellon University
Pittsburgh, PA 15213

ABSTRACT

The growth characteristics of magnetron sputtered Co-22%Cr thin films on amorphous glass or carbon substrates have been investigated utilizing transmission electron microscopy, X-ray diffraction, electrical resisivity and in-plane stress measurements. Results indicate that the initial deposit is "amorphous", but that isolated islands of small crystallites form before the film reaches 5nm film thickness. By 10nm, well oriented grains with hcp c axis perpendicular to the film plane develop, and by 50nm, a twinned columnar microstructure is evident. As this occurs, the in-plane film stress becomes constant. Also, we have observed a distinct subgrain structure in the thinner films (10-50 nm), and this is reflected in the electrical resistivity. This cannot be accounted for by an "evolutionary selection" growth scenario, but must be related to the low surface mobility of adatoms at these low substrate deposition temperatures.

INTRODUCTION

Co-Cr has been studied extensively as the leading candidate for perpendicular (magnetization out of the film plane) magnetic recording media [1,2]. Due to its relatively simple hcp crystal structure, this material also serves as a logical system for the study of microstructural development on various substrates. The development of microstructure in this system has been profusely reported in the literature [3-8]. These studies have indicated a general growth scenario in which an initial fine-grained, randomly oriented "transition layer" first forms, followed by the development of columnar grains, with their c-axes out of the film plane. The thickness of this "transition layer", as well as the morphology of the columns (conically expanding or straight sided) vary according to the particular deposition conditions and/or substrate materials utilized. In this investigation, we have employed transmission electron microscopy (TEM) and X-ray diffraction to examine systematically and in detail the development of microstructure in Co-22 at.%Cr films deposited on glass or amorphous carbon substrates utilizing identical sputtering conditions. In addition, we have measured the in-plane film stress utilizing a laser beam deflection method as well as the electrical resistivity, using a four point probe technique. This data, taken in conjunction with the TEM observations, have revealed results that shed new light on the development of the film microstructure, especially the initial 50nm. These results are compared qualitatively with established models for film growth.

EXPERIMENTAL

Films were deposited onto glass (Dow Corning 7059) or amorphous carbon substrates using a Varian DC Magnetron ("S" gun) sputtering system. Sputtering conditions included an argon pressure of one mTorr, room temperature substrates and a sputtering rate of 0.25 nm/sec. Thin film ($\leq$ 50nm) plan view TEM specimens were prepared by depositing directly onto carbon coated 3mm copper grids, enabling direct TEM observation. Thicker films were deposited onto glass substrates which were mechanically thinned to about 40 microns, after which they were ion (Ar^+) beam milled to electron transparency. Section samples were fabricated by bonding two films face-to-face, mechanical thinning, and ion beam milling. All films were examined using a Philips EM420, operating at 120 kV. In-plane stress measurements were made with a laser beam deflection method [9] in which the substrate curvature due to the film stress is measured. Samples were cut to 0.25" x 1" strips and scanned with the laser, after which the film was removed via etching in aqua regia and the glass substrate scanned again. In this way, the effects of inherent substrate curvature could be removed from the measurement. Electrical resistivity was determined on 0.5 x 2 mm samples employing a four point probe method. These measurements were made at liquid nitrogen temperatures using a current of 100 microamperes to minimize any I^2R heating effects. X-ray

 ©1988 Materials Research Society

rocking ($\Delta\theta_{50}$) curves were taken utilizing CuK_{α} radiation on a Rigaku Geigerflex diffractometer.

EXPERIMENTAL RESULTS

General Microstructure-Plan View

Figures 1a-e show typical plan views of the microstructure for films of thickness 10-500nm. From Figure 1a, it can be seen that by 10nm, a continous film is formed. As the film thickness increases, we observe a mottled contrast for the 50-100 nm films (Figures 1b-c), gradually giving way to a well defined close-packed polycrystalline structure by 200nm (Figure 1d). Also, occasional twins within individual grains (Figure 1e) are observed. As shown in Table 1, the average grain diameter is nearly constant with increasing film thickness , indicating that the final grain size is reached early on, (by 50-100 nm thickness) .Figure 2a shows a plan view of a 5nm film. As shown, the microstructure is primarily "amorphous" (Figure 2b), with occasional clusters of small crystallites (Figure 2c). Electron microdiffraction (EMD) patterns taken utilizing a 10nm probesize (Figure 2d) verify that such regions are indeed crystalline.

TABLE 1. Film Orientation Parameters

t(nm)	d_g (nm)	d_c (nm)	$\Delta\theta_{50}$ (degrees)
10	18.85 (10.13)	----	----
50	19.01 (11.37)	24.38	9.625
100	20.13	16.3-55	9.55
500	20.69	19.5-30.8	6.7

Key: t = film thickness
d_g = average grain diameter
d_c = average column diameter
$\Delta\theta_{50}$ = X-ray rocking curve half width
( ) indicates subgrain diameter

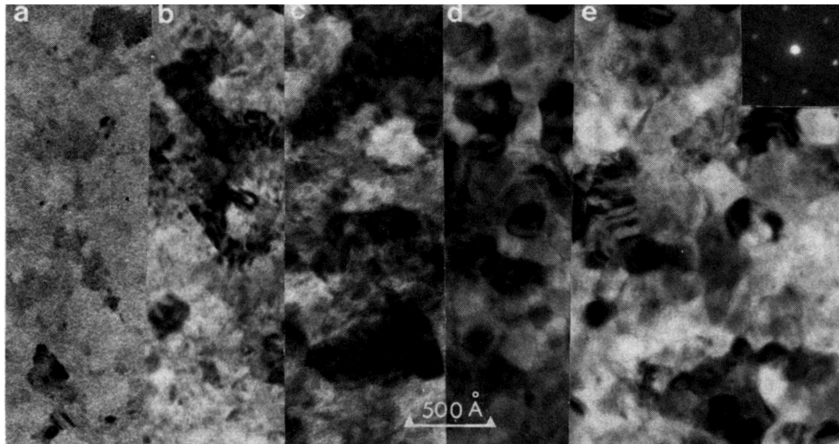

Figure 1. Typical film microstructures at various thickness values (plan view). a) 10, b) 50, c) 100,d) 200,e) 500 nm. Inset in "e" shows a hcp (0001) microdiffraction pattern taken fron a single grain.

Sub-boundary Structure

Close examination of the film microstructure for films less than ~ 50nm (Figure 3a) reveal the presence of boundaries within the grains themselves. Electron microdiffraction patterns (10nm probe size) (Figure 3b) taken across such boundaries reveal a small (<10° about [0001]) misorientation, indicating a low angle grain boundary. This is to be contrasted with EMD patterns taken across the grain boundaries, (Figure 3c), which display misorientations of ~20-30°. The frequency of occurrance of these small angle boundaries decreases with film thickness.By 100-200nm thickness, such boundaries can no longer be distinguished . We believe that these boundaries form to relieve the initial high plastic strains of the growing film.Their presence can also be inferred from both film stress and electrical resistivity measurements, as discussed below.

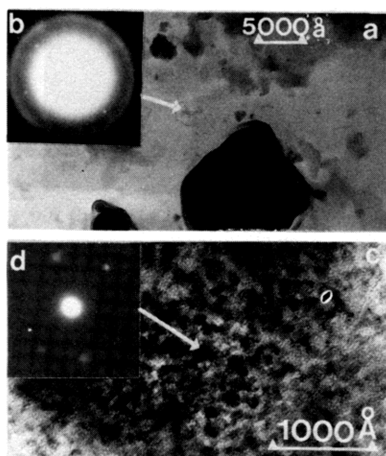

Figure 2. a) Plan view of 5nm film, showing "amorphous" structure and isolated crystallite islands. b) Diffuse ring SAD pattern from this region. c)Detail of island,showing small cyrstallites. d) EMD pattern from individual crystallites.

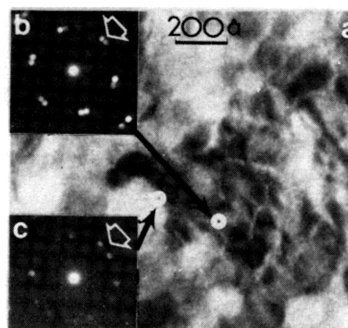

Figure 3. a) Plan view showing intragranular sub-boundary structure. EMD patterns taken across b) sub-grain , c) primary grain boundaries.

Column Structure

In Figures 4a-d are shown sections from films of various thickness. It is interesting to note that at the 10nm thickness, the development of a column structure has not yet commenced, although, as mentioned above, the film displays a strong c axis texture (normal to the film plane). Also, note that the column diameter becomes constant somewhere in the 50-100nm film thickness range (Table 1).One also can observe the development of intragranular twins in this thickness regime. Figures 5a and b show a bright field/dark field pair for a 50nm film. Due to the presence of overlapping grains, it is difficult to unequivocally ascertain if the column is a single grain, however, it appears (Figure 5b) as though this is the case. One should also note that the column daimeters listed in table 1 correspond (within experimental limits) reasonably well to the grain diameters, even at the 50nm thickness. Thus it would appear that the above mentioned subgrains combine to form a single orientation column as the film grows. One will also notice that a well defined "transition layer" is visible in the thinner films (10nm is all "transition layer"), but gradually,becomes indistinct with increasing film thickness, and, at the 500nm thickness, cannot be seen at all (Figure 4d). Thus we get a "back growth" of columns into this layer as the film grows vertically. This is reflected in the observed X-ray rocking curve half widths ($\Delta\theta_{50}$) , also listed in Table 1. This value decreases sharply from 100 to the 500 nm thick films.

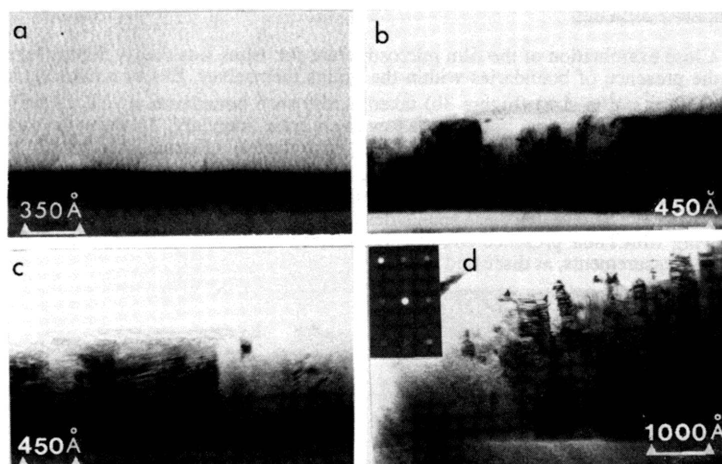

Figure 4. Section views for films of various thickness. a) 10, b) 50, c) 100, d) 500 nm. Inset in "d" shows typical (0110) prism plane pattern.

Twin Structure

As noted previously, by the 50nm thickness, one observes the development of well defined twin structures, both in plan and section views (Figures 6a and b). Electron microdiffraction patterns taken from these regions reveal streaks, due to the intersection of the Fourier shape transform of the thin platelets with the Ewald sphere [10]. Such platelets may well be be either twins or stacking faults. However, from the pattern of Figure 6a inset, the trace of the streaks lies in the $[\bar{1}2\bar{1}0]$ direction, which is consistent with twinning on the $\{10\bar{1}2\}$ plane. This is a common hcp twin plane. If such platelets were stacking faults, they would lie on the (0001) basal plane, and would not yield streaks in the (0002) zone axis of Figure 6a. These twins are thought to form to relieve growth stresses, and appear after a critical film thickness has been attained, beyond which such stresses can no longer be accomodated at the free surfaces. A calculation of such a minimum thickness for twin formation in these materials is currently being performed.

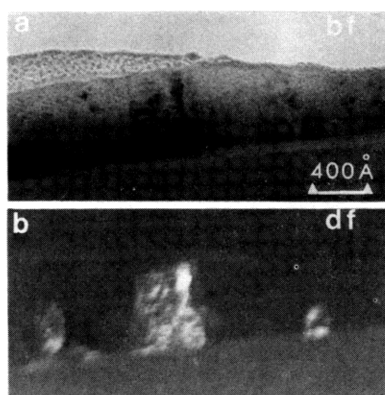

Figure 5. a)BF and b) DF section views, showing single column grains.

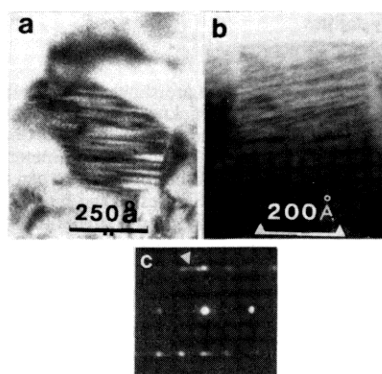

Figure 6. a) Plan and b) section views showing twins. c). (0001) EMD pattern showing streaks due to $(10\bar{1}2)$ twins.

Electrical Resistivity

In Figure 7a , the electrical resistivity is plotted as a function of film thickness. As shown, one observes a sharp increase as one approaches 10nm film thickness. It would be expected that the resistivity would increase with decreasing film thickness due to increased electron scattering from the (now closer) film free surface [10]. However, Figure 7b shows that the product of the resistivity and the film thickness increases as well, indicating an additional contribution to electron scattering in the thinner films. This is thought to be due to the presence of the aforementioned subgrain boundaries in the thinner films, which act as additional electron scattering centers. One will also notice that this value is not observed to change significantly beyond approximately the 100nm thickness. This is consistent with the observation that column boundary widths remain constant with increasing film thickness above this value and/or with a constant density of twins throughout these columns.

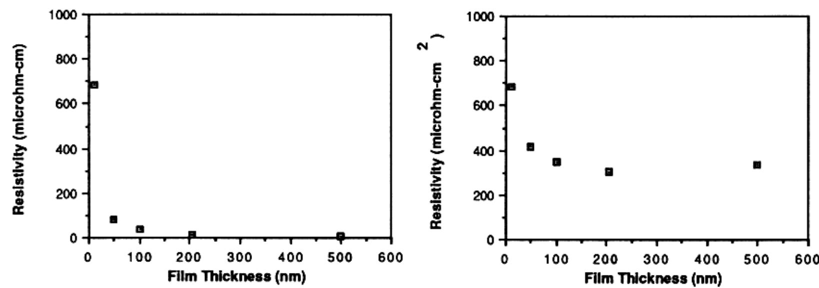

Figure 7. a) Plot showing electrical resistivity as a function of film thickness. b) Resistivity times thickness versus thickness, indicating additional contribution to electron scattering.

Film Stress Measurements

Figure 8a shows the in-plane film stress, computed from experimental measurements of the substrate curvature. Beyond a certain thickness, the film stress reaches a constant value. According to [12], this indicates that the dominant contribution to the stress is caused by the deposition process, and not due to film/substrate effects. This stress was computed from the following relation, as derived in [13]:

$$\sigma = \frac{E_s d_s^2 \kappa_f}{6(1-v_s) d_f} \quad (1)$$

where E_s and v_s are the Young's modulus and Poisson ratio of the substrate, d_s and d_f are the substrate and film thickness, respectively and κ_f is the curvature of the film. In Figure 8b are plotted κ_f and $1/d_f$ versus d_f. These curves intersect at a critical thickness, beyond which the increase in substrate bending fails to keep pace with the increase in film thickness. This value (~100nm) is that at which twins are observed via TEM.These twins can act to relieve growth strains and, as such, can effectively reduce the bending in the film for a given thickness.

DISCUSSION

We now examine the above experimental observations, keeping in mind various proposed models of film growth. Most scenarios proposed for this material [14] involve the formation of a small grained, randomly oriented "transition layer", followed by vertical growth of columns via an "evolutionary selection" mode [15]. This would account for the observed

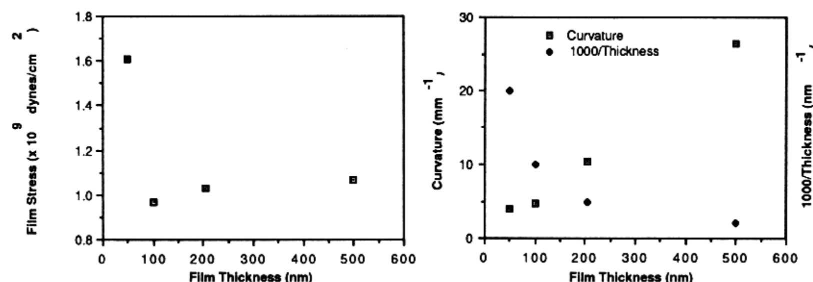

Figure 8. a) Plot of film stress as a function of film thickness. b) Overlay plot of curvature and inverse film thickness as a function of film thickness, showing intersection at a critical value.

long range enhancement of the film texture ($\Delta\theta_{50}$), in the thickest (500nm) films. To account for the presence of well oriented subgrains and strong texture in films as thin as 10nm, however, we must consider other effects. According to Grovenor et al [16], when the substrate temperature is less than one-third of the melting point of the metal being deposited, the mobility of adatoms is low and incoming deposit atoms "stick" where they land. This is seen to lead to the development of fine grains collected into "bundles" of approximately the same orientation (as per Figure 3a). They further propose that, in this thickness range, small groups of atoms crystallize from a precursor (amorphous) phase, releasing a heat of crystallization which further stimulates crystallization until neighboring nuclei impinge. Thus the grain size attained is dependent on the density of the crystallite nuclei. This would also be consistent with the existence of a tensile stress in such films, since the precursor to crystalline transformation involves a volume decrease for most metals. This volume change is constrained by the substrate so that the deposit is in tension and the substrate in compression. Based on experimental observations, this critical thickness appears to be on the order of 5nm. The thin films posess a high plastic stress, which can give rise to the formation of subboundaries. With increasing film thickness, the stress is relieved by the formation of twins, enabling the elimination of these boundaries. This is supported by the above electrical resistivity measurements.

SUMMARY

Experimental results have yielded the following characteristics of the growth of Co-Cr thin films on amorphous substrates. The initial film deposit is prodominently amorphous, with occasional islands of small crystallites forming by 5nm thickness. By 10nm, the film is entirely polycrystalline and already well c-axis textured. At this thickness, one observes distinct intragranular low angle boundaries within the primary grains. A column structure has not yet developed. This is reflected in the anomously high electrical resistivity values for these films. In-plane tensile stresses are high. By 50nm, well developed columns are seen in which one observes ($10\bar{1}2$) twins. At this thickness, the in-plane stress begins to level off to a constant value. Subgrain structures are still evident. By 100nm, these are all but gone and the electrical resistivity follows a normal thickness dependence. Further growth is essentially all vertical, giving rise to a sharp decrease in the X-ray rocking curve width by 500nm.

Film growth scenarios based on evolutionary selection do not account for the observed microstructures in the thinnest films, and one must take into account the low surface mobility of adatoms at these low deposition temperatures.

ACKNOWLEDGEMENTS

Funding for this work was provided by the Magnetic Materials Research Group at Carnegie-Mellon University, through a Grant from the Division of Materials Research, National Science Foundation, Grant No. DMR-8613386.

REFERENCES

1) Iwasaki, S. and Nakamura, Y., IEEE Trans. Mag. MAG-13 (5), 1272 1977.
2) Weilinga, T., PhD Dissertation, Twente Univ. of Tech., Enschede, The Netherlands 1983.
3) Hergt, R., Pfeiffer, H. and Fritzch,L., Phys. Stat. Sol. (a) 98, 69 1986.
4) Grundy, P.J., Ali, M. and Faunce, C. A., IEEE Trans Mag., MAG-25 (5), 794 1984.
5) Futamoto, M., Honda, Y., Kakibayashi, H., Shimotsu, T. and Yoshida, K., Jap. Jl. Appl. Phys. 24 (6), L460 1985.
6) Hwang, C., Laughlin, D.E., Mitchell, P.V., Layadi, A., Mountfield, K.R., Snyder, J. and Artman, J.O., J. Magn. Mag. Mat., 54-57 , 1676 1986.
7) Lee, J. W., Demczyk, B.G., Mountfield, K.R., and Laughlin, D.E., J. Appl. Phys., 61 (8), 3813 1987.
8) Lee, J.W., Demczyk, B.G., Mountfield, K.R.and Laughlin, D.E., IEEE Trans. Mag., MAG-23 (5), 2455 1987.
9) Young, D.W., Ho, H., Bauer, C.L., Mahajan, S. and Milnes, A.G., Proc. 1988 MRS Spring Mtg.
10) Edington, J.W., Practical Electron Microscopy in Materials Science, Van Nostrand Reinhold Co., N.Y. 1976, p 83.
11) Sondheimer, E.H., Adv. Phys.,1 ,1 1952.
12) Klockholm, E. and Berry, B.S., J. Electrochem. Soc., 824 1968.
13) Hoffman, R.W., in Physics of Thin Films, G. Hass, ed., Academic Press, N.Y., 3, 211 1966.
14) Byun, L., Silverstein, J.M., and Judy, J.H., unpublished research.
15) Van der Drift, A., Philips Res. Rpts.,22, 267 1967.
16) Grovenor, C.R.M.,Hentzell, H.T.G. and Smith, D.A., Acta. Met., 32 (5), 773 1984.